Available online at www.sciencedirect.com
SCIENCE DIRECT®
Journal of Molecular Graphics and Modelling 23 (2004) 175–187
Journal of Molecular Graphics and Modelling
www.elsevier.com/locate/JMGM

Computational analysis of tyrosine phosphatase inhibitor selectivity for the virulence factors YopH and SptP

Xin Hu, Milos Vujanac, C. Erec Stebbins*

Laboratory of Structural Microbiology, The Rockefeller University, 1230 York Avenue, New York, NY 10021, USA

Received 1 March 2004; received in revised form 20 May 2004; accepted 26 May 2004

Available online 15 July 2004

Abstract

Bacterial pathogens such as *Yersinia* and *Salmonella* represent an important medical concern, causing human diseases ranging from gastrointestinal disease to the plague. The development of novel treatments of these bacterial infections has gained high priority recently due to the emergence of antibiotic resistance in these pathogens and the threat of the use of microbial agents as biological weapons. YopH of *Yersinia* and SptP of *Salmonella* are virulence factors that belong to the family of protein tyrosine phosphatases (PTPs). A great challenge remains in the design of selective PTPs inhibitors due to their highly conserved active site. In this paper, we present a comparative docking study to probe the selective inhibition of YopH and SptP with PTP1B in order to better understand their binding interactions with the bacterial tyrosine phosphates. Characterized binding sites in PTP1B were compared with YopH and SptP. Molecular dynamics simulations were used to incorporate ligand-induced conformational changes in the binding sites. These results, together with those binding modes and binding affinities distinguished in individual PTPs, provide insight into the structure-based design of inhibitors for YopH and SptP.

Keywords: Protein tyrosine phosphatases (PTPs); YopH; SptP; PTP1B; Docking; Virtual screening

1. Introduction

Pathogenic bacteria such as *Yersinia* spp. and *Salmonella* spp. represent an important human health concern. *Yersinia* spp. are causative agents of diseases ranging from gastrointestinal syndromes to the plague [1]. *Salmonella* cause a variety of diseases such as typhoid fever and food poisoning, and are responsible for over one billion new human infections each year [2]. The emergence of antibiotic resistant strains of *Yersinia* and *Salmonella*, as well as the risk these agents pose as biological weapons, have made the development of novel therapeutics against these organisms a high priority [3–5].

These two pathogenic bacteria share a common virulence mechanism, termed a type III, or "contact dependent" secretion system, that confers the ability to translocate bacterial proteins into the host cell cytosol [6]. *Yersinia* secrete six virulence factors referred to as *Yersinia* outer proteins (Yops) [7]. One of these, YopH, belongs to the family of protein tyrosine phosphatases (PTPs), acting on target pTyr-containing proteins within infected eukaryotic cells to disrupt the normal cytoskeletal structure and regulation [8]. Interestingly, *Salmonella* also translocates a virulence factor with PTP activities into host cells. This protein, called SptP, exists as a bifunctional, multidomain protein, and functions in part to restore host cell cytoskeletal structure disrupted by the internalization process. The C-terminal domain of SptP is similar to the *Yersinia* tyrosine phosphatase YopH as well as to eukaryotic tyrosine phosphatases [9,10].

The fact that *Yersinia* and *Salmomella* possess virulence factors with PTP activity suggests a novel strategy of antibacterial intervention. In general, PTPs have emerged as a promising class of drug targets exemplified by PTP1B, inhibitors of which act as effective therapeutics for the treatment of type II diabetes, insulin resistance, and obesity, and has triggered an extensive study on the structure-based drug design in last decades [11–14]. The wealth of PTP1B inhibitors, some of which have already progressed into clinical trials, provides a valuable resource for the design of specific YopH and SptP inhibitors.

A key point in the design of PTP inhibitors is to achieve selective inhibition, which is complicated by the highly conserved catalytic site contained in these enzymes [15,16]. The conformational changes of the so-called WPD loop in the active sites of PTPs are crucial to ligand binding and pose a challenging problem in the applications of computer-aided

* Corresponding address. Tel.: +1 212 327 7190; fax: +1 212 327 7191.
E-mail address: stebbins@rockefeller.edu (C. Erec Stebbins).

1093-3263/$ – see front matter © 2004 Elsevier Inc. All rights reserved.
doi:10.1016/j.jmgm.2004.05.004

modeling techniques [17]. Studies of PTP1B inhibitors reveal that, in addition to the catalytic pTyr active site, other residues also provide unique structural opportunities for achieving inhibitor selectivity. These structural features in PTP1B include the second phosphate binding site, the YRD signature motif, and the gateway residue glycine (Gly)259 [18].

Herein, we report a comparative docking study of YopH of *Yersinia* and SptP of *Salmonella* with eukaryotic protein tyrosine phosphatase PTP1B. The focus of the study is to identify structural features in YopH and SptP binding sites that can be used for structure-based drug design. Molecular dynamics simulations were used to incorporate ligand-induced conformational changes, which are generally restricted in most approaches to molecular docking. The use of high throughput docking in the database screening for selective PTP inhibitors is also discussed.

2. Methods

2.1. PTP inhibitors

We selected six compounds from known PTP1B inhibitors to be used as probes in the comparative docking study (Fig. 1). The six compounds represent those typical structures that are frequently encountered in the design of PTP1B inhibitors as well as other PTP inhibitors. Both the crystal structure of PTP1B in complex with these compounds and experimental inhibition data (K_i) are available (Table 1). These compounds are chemically diverse, but generally contain a pTyr mimetic capable of binding into the catalytic site of PTPs. Compound VI is the most potent PTP1B inhibitor reported so far with $K_i = 1.8$ nM. It also have a relatively high activity against YopH ($IC_{50} = 3.0\,\mu M$) [19,20]. In addition, compound IV is a general PTP scaffold inhibitor [21] and compound I and II display inhibitory activity against a broad range of PTPs [22,23]. Therefore, these selected compounds are potential inhibitors for YopH and SptP, and are informative in a modeling study to probe the structural characteristics of the two bacterial protein tyrosine phosphatases.

Table 1
Estimated binding free energies (kcal/mol) of compounds I–VI in PTP1B, YopH, and SptP predicted by AutoDock 3.0

Compound	ΔG (PTP1B)*	ΔG (YopH)	ΔG (SptP)	pK_i**	Reference
I	−11.87 (4.31)	−10.12	−8.62	4.80	[22]
II	−12.86 (0.82)	−12.45	−10.04	5.29	[23]
III	−14.50 (1.64)	−12.11	−10.69	6.22	[30]
IV	−10.70 (0.56)	−10.17	−8.92	4.41	[21]
V	−14.76 (1.17)	−11.58	−8.04	7.66	[21]
VI	−15.86 (2.14)	−12.59	−11.02	8.74	[19,20]

* The root-mean-square deviations (RMSD) of docked compounds in PTP1B are given in parentheses. RMSD is computed between the docked conformation and experimental geometry of PTP1B X-ray structure.

** Inhibitory activities against PTP1B.

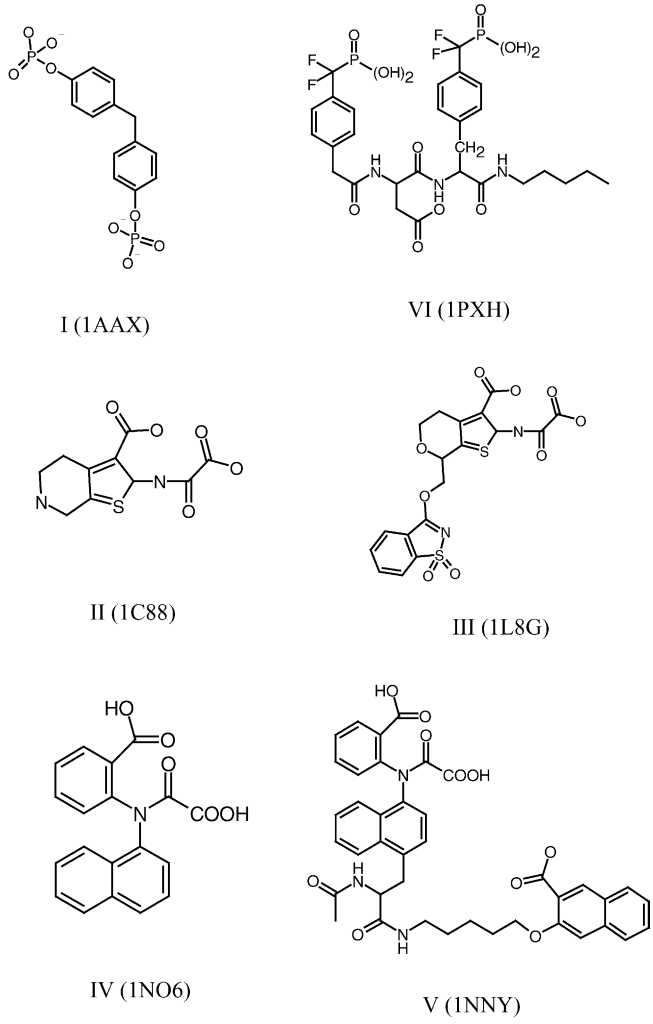

Fig. 1. Selected compounds in the docking study. The corresponding protein structures with PTP1B (pdb entry) are given in parenthesis.

A focused library was also built to examine the ability of high throughput docking for selective PTP inhibitors. Five thousand compounds were collected with molecular weight ranging from 250 to 500. Twenty-five known PTP1B inhibitors, including the six probes, were added to the database. The potencies (K_i or IC_{50}) of these PTP1B inhibitors range from 10 nM to 100 μM. We cannot guarantee that all 5000 compounds are inactive to PTPs. These were selected randomly from our in-house database of over 3,000,000 compounds, and those with known PTP mimetics were excluded. The probability of compounds with activity to PTPs in micromolar range is expected to be very low, and our selection is thus suitable to be used as a background set for testing.

2.2. Docking

The Sybyl 6.9 package [24] was used to prepare the ligand and protein data required in docking. The atomic coordinates of PTP1B, YopH, and SptP used in this study

were obtained directly from the protein data bank [25]. The hetero atoms (cofactors, water molecules, and ligands) were removed. Polar hydrogens were added and Kollman charges were assigned to protein atoms. Desolvation parameters were assigned using the ADDSOL module of AutoDock [26]. The structures of six compounds were extracted from the PTP1B/ligand complexes. All hydrogen atoms were presented and a short minimization (100 steepest descent steps with Tripos force field) was performed to release internal strain. Partial charges were assigned to the atoms according to the method of Gasteiger and Marsili [27]. The AUTOTORS module of AutoDock defined the active torsions for each docked compound.

The automated molecular docking calculations were carried out using AutoDock 3.0 [26]. The active site of the protein was defined using AutoGrid. The grid size was set to 90 × 90 × 90 points with a grid spacing of 0.375 Å centered at the center of mass of the ligand. The Lamarckian genetic algorithm (LGA) was used as search method. Each LGA job consists of 100 runs, and the number of generation in each run was 27,000 with an initial population of 50 individuals. The maximum number of energy evaluations was set to 1,000,000. Operator weights for crossover, mutation, and elitism were 0.80, 0.02, and 1, respectively. The rest of the parameters were set as the default values. Results differing by less than 1.5 Å in positional root-mean-square deviation (RMSD) were clustered together and represented by the result with the most favorable free energy of binding.

After docking, the complexes were energetically minimized permitting only the ligand and the sidechain atoms of the protein to relax. Energy minimizations were carried out employing Sybyl 6.9. In each step, MMFF94 force field was applied with 0.05 kcal/Å convergence and 5000 steps using the Powell method.

2.3. Molecular dynamics simulations

The molecular dynamics simulations were conducted using Sybyl 6.9. All the starting structures of PTPs (apo or with ligand) were first subjected to minimization. The Asp residue on WPD loop was assigned a protonated form consistent with its role in acting as proton donor. Only atoms within 20 Å of the catalytic cysteine were allowed to move, and the duration of the simulation was set to 1 ns. The non-bonded pair list was updated every 25 steps. The time-step used was 2 fs and a snapshot was taken every 1 ps. The temperature of the simulations was maintained at 300 K using the weak coupling method with a coupling time of 100 fs. Bond lengths involving hydrogen atoms were constrained using the SHAKE algorithm [28]. The cutoff of non-bonded interactions was set to 8 Å. The molecular mechanics force field MMFFs was used for the simulation system and MMFF charges were assigned for protein and ligand. The system was solvated with a water layer using a pre-computed solvent box in Sybyl 6.9. Dynamic analysis was performed using MSS module in Sybyl 6.9. An ensemble of MD conformations (500) was exported to a Sybyl database and further used as docking targets by AutoDock for interesting compounds.

2.4. High throughput docking

High throughput docking was carried out using FlexX 1.10 [29]. The program was installed on a 32-processor linux cluster. Standard docking conditions of the FlexX program were used. Generally, a receptor description file was defined from the PDB coordinates of protein target through the FlexX graphics interface. The active site includes protein residues in a 10 Å radius sphere centered on the conserved residue Cys215 (PTP1B number). Formal charges were assigned for the ligand. The original FlexX scoring function was used and the top 30 poses for each compound were retrieved.

The enrichment was used to measure the quality of the screening results. It is defined as:

$$\text{enrichment} = \frac{a/n}{A/N}$$

where N is the number of compounds, n is some predetermined number of compounds to be screened, A is the number of actives in the entire collection, and a is the number of actives in the top n ranked compounds. Enrichment over 1% or 2% of the total compounds is generally used.

3. Results

The six compounds were first re-docked to their corresponding PTP1B structures using AutoDock 3.0, with the aim to test the AutoDock program for its docking accuracy and reliability in reproducing the crystallized binding geometry of PTP inhibitors. Subsequent docking of these probes to YopH and SptP was performed using the same procedure. The predicted binding modes and the corresponding binding energies estimated by AutoDock scoring function were examined with comparison to that observed in PTP1B. The results are shown in Table 1. Characterized interactions observed for each compound in the three PTP targets are summarized in the following section.

3.1. Compound I

Compound I is a typical phosphotyrosine (pTyr) PTP inhibitor featured with two phosphate functionalities. Two binding modes were observed in the X-ray crystal structure [22]. The docking results showed that the conserved interactions of the proximal phosphate group in the catalytic binding site and the typical “sandwich” π–π stacking interactions with residues Phe182 and Try46 were predicted correctly, but the docked conformation adopted a binding mode that differed from those in the crystal structure. As shown in Fig. 2A, the distal phosphate group of compound I pointed directly to the second phosphate binding

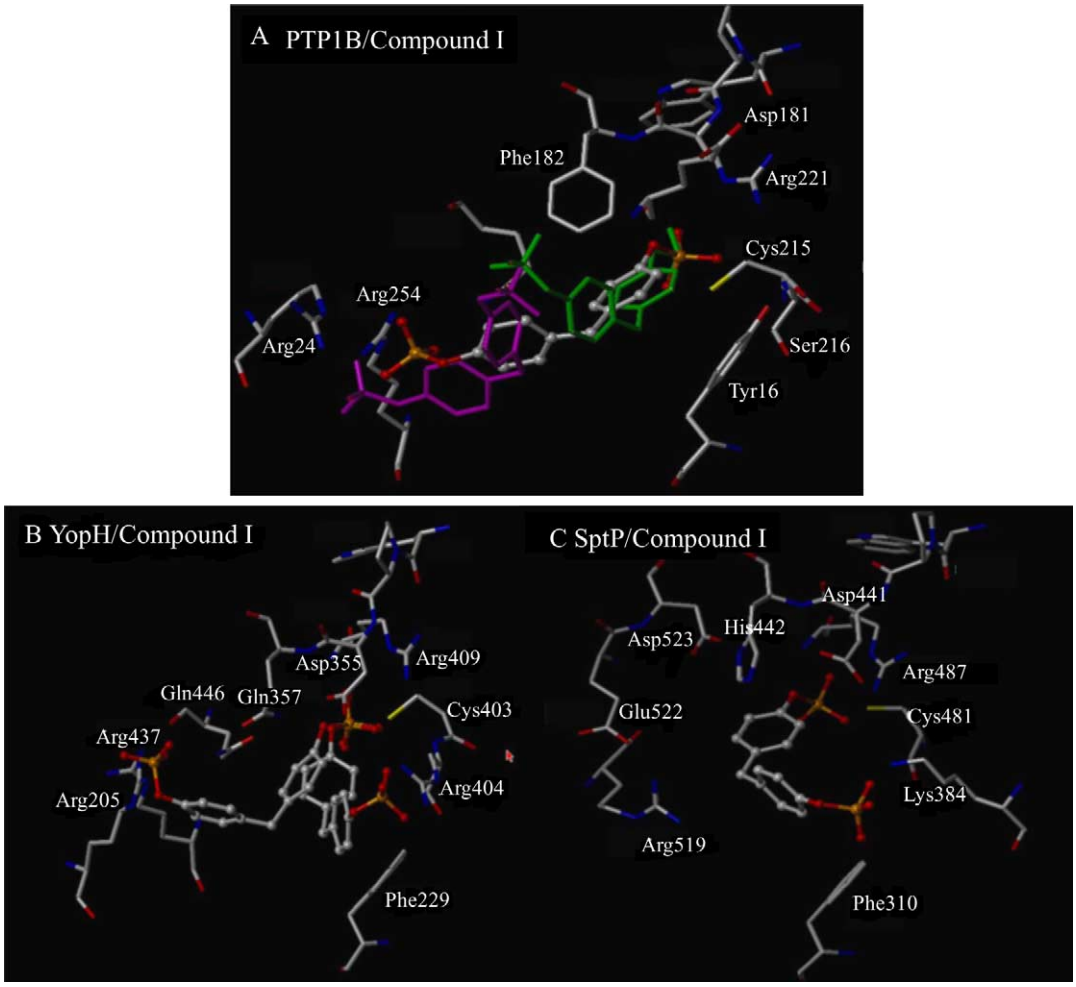

Fig. 2. (A) Superposition of docked conformation of compound I (ball and stick, CPK) with the two experimental conformations (stick, green and magenta) in the crystal structure in PTP1B; (B) two binding modes of compound I in YopH; and (C) the binding of compound I in SptP.

site of PTP1B, forming strong charged interactions mainly with Arg24 and Arg254. This binding mode preferred by AutoDock can be inferred from the estimated binding energies (−11.87 kcal/mol). In contrast, the binding energies of the two native conformations estimated by AutoDock scoring function are only −9.75 kcal/mol and −7.23 kcal/mol, much higher than that of the docked conformation.

The highest resolution structure of YopH (1lyv) was used in the docking of compound I to YopH. The predicted binding mode was very similar to that in PTP1B: the proximal phosphate bound to the catalytic pTyr pocket, while the distal phosphate group pointed to an adjacent region forming interactions with residues Arg205 and Arg437 (Fig. 2B). These results suggest that YopH, like PTP1B, also possesses a second binding site featured with two arginine residues that is capable of accommodating an aryl phosphate group. The estimated binding free energies of compound I in YopH are −10.12 kcal/mol, about 1 kcal/mol higher than that in PTP1B. This is most probably because the “sandwich” stacking interactions are lost in YopH, since a residue Gln357 is present at the position of PTP1B Phe182. Interestingly, an alternative binding mode of compound I in YopH was also observed with approximately the same estimated binding energies (−10.03 kcal/mol). As illustrated in Fig. 2B, the distal phosphate group formed van der Waals contacts and ionic interactions with residue Arg404, which is specific to YopH. Such a binding mode was not found in PTP1B because Ser216 is present at this position, and lacks the capability to form similar interactions.

Docking compound I to SptP resulted in several binding modes different from that observed in PTP1B and YopH. The distal phosphate group was found to interact with various residues flanking the pTyr binding pocket. However, all these docked conformations showed weak interactions with estimated binding energies of 3–5 kcal/mol higher than that in PTP1B and YopH, suggesting that compound I is less selective to SptP. Fig. 2C shows the most energetically stable conformation of compound I bound in SptP (−8.62 kcal/mol), in which the distal phosphate group interacts with Lys384. The favorable binding mode to a characterized second phosphate binding site found in PTP1B and YopH was not observed

in SptP. In addition, a neutal and nonploar residue Leu482 replaced the characterized residue Arg404 in YopH, but the potential "sandwich" stacking interactions commonly found in mammalian PTPs were recovered by residue His442 in SptP.

3.2. Compound II

Compound II is a derivative of 2-(oxalyl-amino)-benzoic acid (OBA), a general pTyr mimetic commonly used in the design of PTP1B inhibitors [23]. The selectivity of compound II to PTP1B is achieved through two important interactions: one is the forming of an unique hydrogen bond between the basic nitrogen of OBA and the carboxylic group of Asp48 from the signature motif YRD. The other is that of the *ortho*-carboxylate group forming a charged interaction with NH^+ of Lys120. AutoDock was successful in reproducing the experimental binding mode with RMSD of 0.82 Å (Fig. 3A). Key interactions with Asp48 and Lys120 were well preserved in the docked conformation.

Initially, docking compound II to the high resolution structure 1lyv failed due to steric hindrance at the pTyr binding pocket. To take into account protein flexibility, we docked compound II to several other available YopH structures. Successful docking was obtained with the protein structure 1ytw. In addition to significant conformational changes of WPD loop in structure 1ytw, this docking reveals that residue Asp230 adopts a favorable conformation for hydrogen bonding with the nitrogen of compound II (Fig. 3B). However, the *ortho*-carboxylate group of compound II interacts with Arg404 in YopH by forming strong charged interactions with the guanidinium side chain. The interaction with Arg404 in YopH appears stronger and more extensive than the corresponding binding of PTP1B Lys120 at this position. This can be seen from the predicted binding free energies, which are comparable to PTP1B (−12.45 kcal/mol), although YopH lacks the "sandwich" stacking interactions.

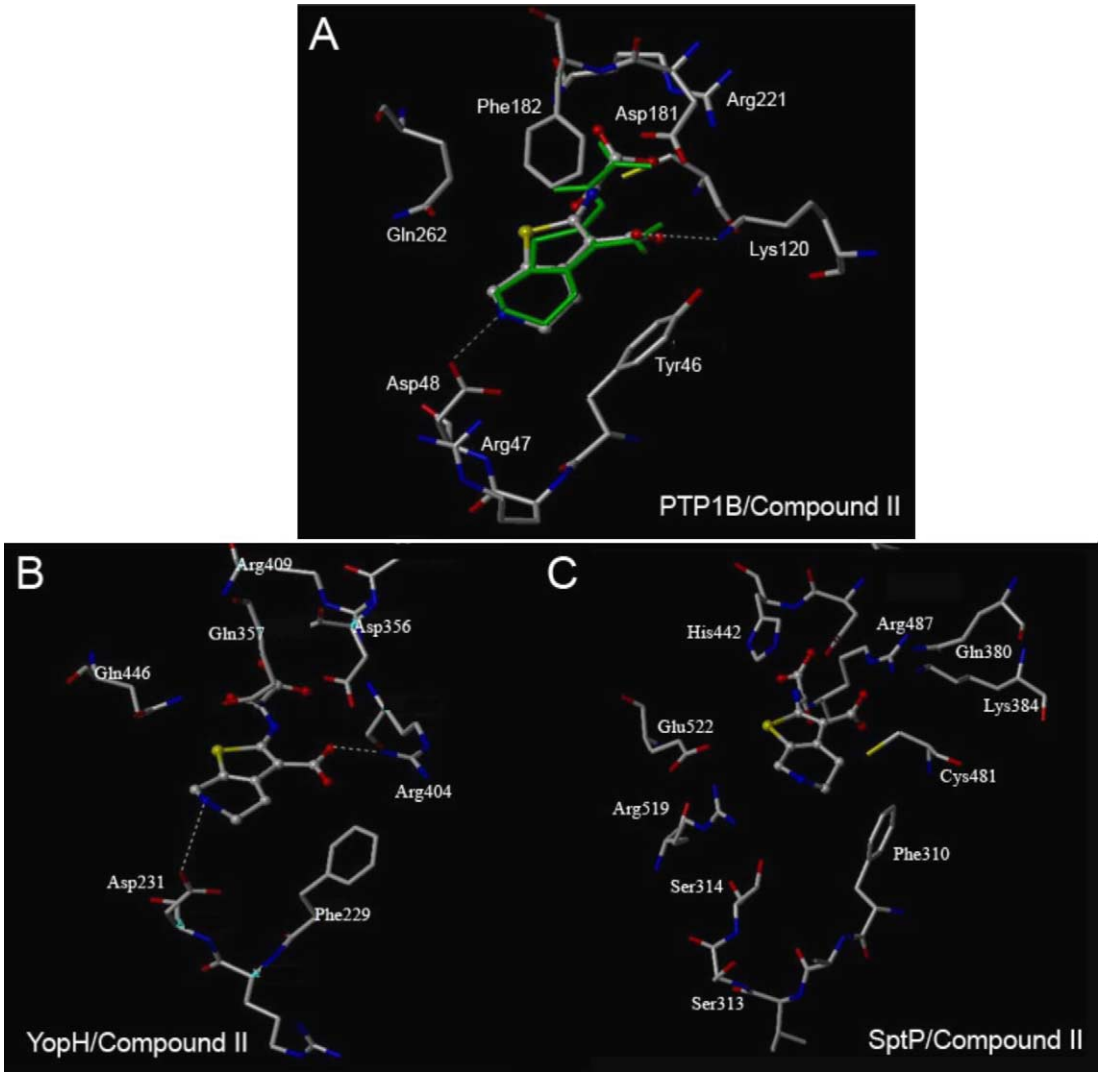

Fig. 3. (A) Superposition of docked conformation of compound II (ball and stick, CPK) with the experimental conformation (stick, green) in the crystal structure in PTP1B; (B) the binding of compound II in YopH; and (C) the binding of compound II in SptP.

Compound II binds differently in SptP. Compared to PTP1B and YopH, the OBA group inserts more deeply into the pTyr pocket. Two uncharged residues in SptP, Ser313 and Ser314, occupy the position of the signature motif Arg47 and Asp48 in PTP1B. The specific interactions between the carboxylate group of Asp and the basic nitrogen of OBA were not observed for SptP. The distance between the nitrogen and the hydroxyl oxygen of Ser314 is 5.1 Å, too far to actually involve any interactions (Fig. 3C). Molecular dynamics simulations show that the guanidinium group of Arg519 formed stable hydrogen bonds with Glu522 and Ser314, making the hydroxyl group of Ser314 inaccessible to the piperidine ring of compound II. Using a multiple conformation docking strategy, compound II was docked to an ensemble of 500 MD conformations of SptP. No favorable conformation of compound II was observed to interact with residue Ser314.

3.3. Compound III

Compound III is a derivative of compound II with a side group of saccharin. The sulfone oxygens in the saccharin group bind to the backbone carbonyl of Asp48, a carbone atom in Gly259, and the sulfur atom in Met258. Such interactions at the so-called "258/259 gateway" are favorable to PTP1B since a more bulky residue is present at position 259 in many other PTPs, causing steric hindrance to reach the second phosphate binding site [30]. Fig. 4A shows the superposition of the AutoDock-generated conformation with lowest binding energies of −14.50 kcal/mol and RMSD of 1.64 Å to the experimental structure of compound III.

Compound III binds to YopH with a similar binding mode as in PTP1B (Fig. 4B). Besides the conserved interactions at the catalytic binding site, the saccharin group is capable of binding to the second phosphate binding site and forming charged interactions and hydrogen bonding with Arg205 and Gln446. This also causes the guanidinium group of Arg205 to move away from the pTyr binding pocket. Gly442 occupies a similar position to PTP1B Gly259, allowing the saccharin group easier access to the second phosphate binding site. The estimated binding energies of compound III to YopH are −12.11 kcal/mol, about 2.0 kcal/mol higher than that in PTP1B. The decreased binding energies might be due to the lack of "sandwich" stacking interactions in YopH, or the differing molecular surface properties of the second phosphate binding site.

The interaction of compound III in SptP is shown in Fig. 4C. Instead of binding to a second phosphate binding site, the sacchrin group of compound III was found to point to a region defined by residues Phe310, Arg309, and Gln385, forming extensive hydrogen bonding, van der Walls contacts, and π–π interactions. As a result, the OBA group adopted a conformation in the active binding site opposite to the modes as observed in PTP1B and YopH. While the amino-oxalyl group formed similar interactions with the conserved Arg487 and Asp441, the *ortho*-carboxylic acid pointed to the opposite side forming hydrogen bonds with Arg519. The estimated binding free energies of compound III in SptP are only −10.69 kcal/mol, indicating that such a "reverse" binding mode of OBA at the pTyr binding site is less favorable.

3.4. Compound IV

The PTP1B structure in complex with compound IV naphthyloxamic acid retains an open form similar to the unoccupied enzyme. This is different from most other PTP1B inhibitors, which induce conformational changes of the WPD loop of the protein which closes the active site pocket [21]. Docking compound IV to the native PTP1B structure (1no6) reproduced the experimental geometry satisfactorily, giving an RMSD of 0.58 Å and estimated binding energies of −10.70 kcal/mol. The carboxylic acid interacted with the conserved Arg221, and the amino benzoic acid formed hydrogen bonds with Cys215 and the backbone residues of WPD loop (Fig. 5A).

Since a closed form of YopH precludes the bulky naphthyloxamic acid binding into the pTyr binding pocket, we used the open structure of YopH 1ypt as docking target. The dominant binding mode of compound IV in YopH adopted a very similar binding mode to that in PTP1B (Fig. 5B). The estimated binding energies were approximately the same as in PTP1B (−10.17 kcal/mol), indicating that naphthyloxamic acid is a general nonselective PTP inhibitor. Moreover, besides the docking in the active pocket, several other interesting binding modes were also observed. As shown in Fig. 5B, one was found at a site around the FDR motif. The naphthalene and the carboxylic group made an extensive hydrophobic interaction and hydrogen bonding with residue Arg230, Asp231, and Lys225. The other two binding modes were oriented towards two pockets in the second phosphate binding site, predominantly driven by strong charged interactions with residue Arg205. Analysis showed that these two pockets possess a different shape and charge distribution, but both have good complementarity to the functionality group. Interactions of compound IV at these putative sites, which are not apparent in PTP1B, revealed distinct structural differences between YopH and PTP1B at the proximal region.

The available structures of SptP to date possess a closed conformation of WPD loop [10]. AutoDock failed to generate a conformation of naphthyloxamic acid bound in the active pocket due to the steric clash. In order to achieve a successful docking, we constructed an open structure of SptP by adjusting the WPD loop based on alignment with YopH (1ypt) and used in the docking of compound IV. As expected, this resulted in a binding mode of compound IV in SptP very similar to those in PTP1B and YopH (Fig. 5C). The compound was stabilized in the active site by hydrogen bonding and hydrophobic interactions with conserved residues. Molecular dynamics simulations showed that the active binding pocket remains an open form in complex with naphthyozamic acid, as was observed in PTP1B and YopH

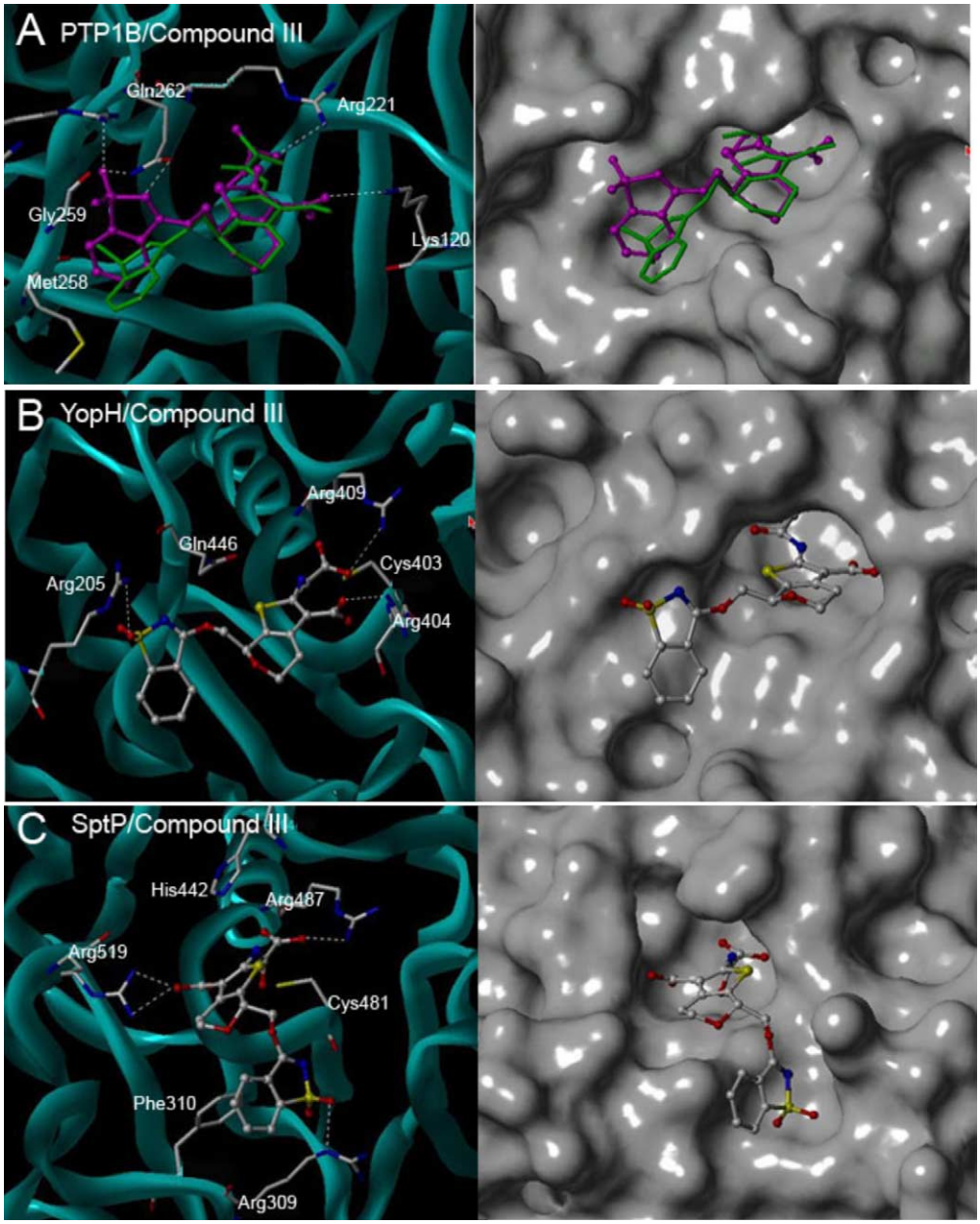

Fig. 4. The binding modes of compound III in PTPs. The protein surface is shown on the left. (A) Superposition of docked conformation of compound III (ball and stick, magenta) with the experimental conformations (stick, green) in the crystal structure in PTP1B; (B) the binding of compound III in YopH; and (C) the binding of compound III in SptP.

dynamics simulations. This contrasted to other compounds, in which the WPD loop moved toward the active site and closed the pocket upon ligand binding.

3.5. Compound V

Compound V is derived from compound IV by attaching an additional group naphthoic acid to access the second phosphate binding site. The binding mode of compound V in PTP1B predicted by AutoDock was in good agreement with the experimental conformation, with an RMSD of 1.17 Å and estimated binding energies of −14.76 kcal/mol (Fig. 5D). The attached naphthoic acid carboxylate participated in charged interactions with Arg24 and Arg254 at the second site, making contributions to a 25-fold increased potency and a significant improvement of selectivity [21].

Three binding modes of compound V bound in YopH were observed (Fig. 5E). Besides the naphthyloxamic acid docked in the active binding pocket, the naphthoic acid was found to point to three distinct sites forming both ionic and van der Waals contacts with surrounding residues. The naphthoic acid was held in the two pockets around the second phosphate binding site. In the third binding mode, the naphthoic acid bound to a region defined by the FRD motif and

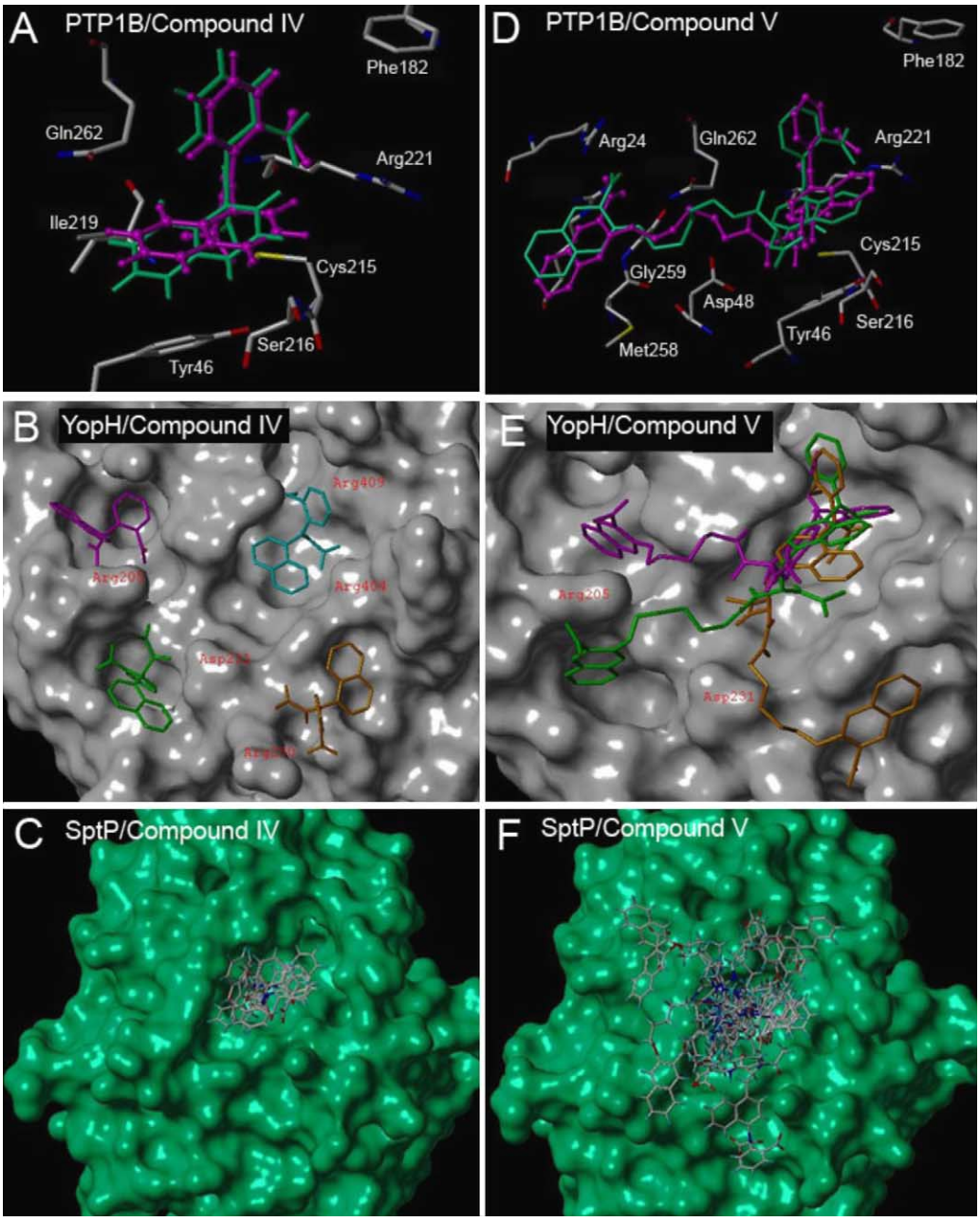

Fig. 5. The binding modes of compound IV and compound V in PTPs: (A) superposition of docked conformation of compound IV (ball and stick, magenta) with the experimental conformation (stick, green) in the crystal structure in PTP1B; (B) the binding of compound IV in YopH; (C) the binding of compound IV docked in SptP; (D) superposition of docked conformation of compound V (ball and stick, magenta) with the experimental conformation (stick, green) in crystal structure in PTP1B; (E) the binding of compound V in YopH; and (F) representative clusters of compound V docked in SptP.

Lys225. It is worth noting that these binding modes agree well with the docking results of compound IV. Therefore, YopH inhibitors could also be achieved by tethering fragments such as naphthyloxamic acid and naphthoic acid with an appropriate linker, an efficient approach used in the design of PTP1B inhibitors [21].

The open structure of SptP was used in the docking of compound V, which predicted several clusters with binding energies generally higher than −8.0 kcal/mol (Fig. 5F). Visual inspections of these docked conformations suggested that none of these binding modes was energetically stable. Using the multiple conformation docking combining with molecular dynamics, an ensemble of 500 MD conformations of SptP were sampled. Compound V was docked to these MD snapshots and the most stable conformations of docked protein complexes were analyzed. Fig. 5F shows some AutoDock-generated conformations extracted from these multiple conformation docking. It can be seen the second group naphthoic acid clustered on the protein surface with a number of weakly non-specific interactions.

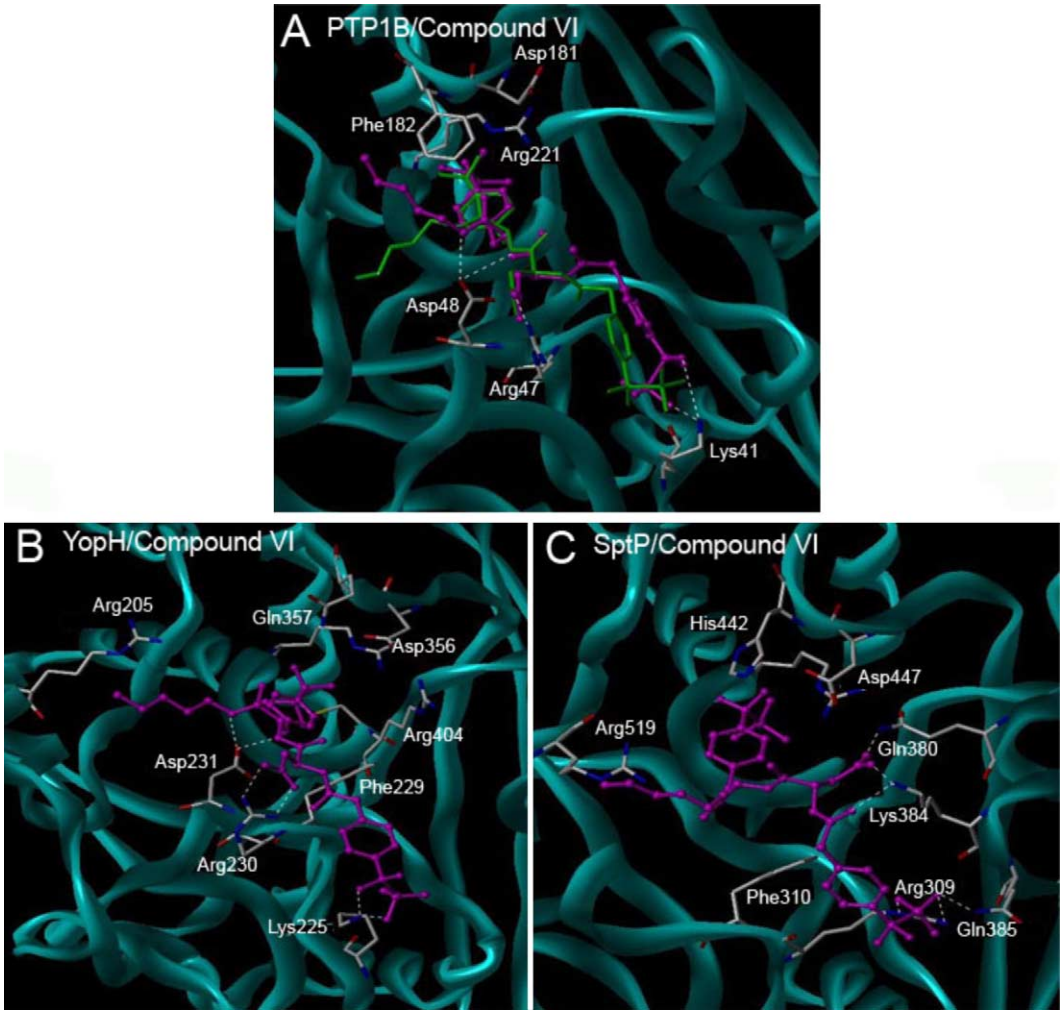

Fig. 6. (A) Superposition of docked conformation of compound VI (ball and stick, magenta) with the experimental conformation (sticks, green) in the crystal structure in PTP1B; (B) the binding mode of compound VI in YopH; and (C) the binding mode of compound VI in SptP.

3.6. Compound VI

The X-ray structure shows that compound VI binds to PTP1B at a proximal region defined by residues Lys41, Arg47, and Asp48, where it undergoes significant conformational changes due to the ligand binding [19]. Re-docking compound VI back to its native protein structure (1pxh) generated a conformation with an RMSD of 2.14 Å and estimated binding energies of −15.86 kcal/mol. Fig. 6A shows the superposition of docked conformation with the X-ray structure of compound VI in PTP1B.

Compound VI was docked to an ensemble of multiple conformations of YopH to take into account protein flexibility at the proximal region. As expected, compound VI interacted with YopH in a manner similar to that in PTP1B. The distal 4-phosphonodifluoromethyl phenylacetyl group made both van der Waals and ionic contacts with Arg231 and Lys225 (Fig. 6B). To enable these interactions, residue Arg231 moved toward the active site, forming hydrogen bonds with the carboxylate group of compound VI, while residue Lys225 moved oppositely to the active site to interact with the distal phenylacetyl group. Other arrangements were also observed with residues Asn293, Leu263, and Arg295. These conformational changes are crucial to the success of docking and are only apparent after multiple conformations are sampled. The estimated binding energies of compound VI in YopH are −12.59 kcal/mol, about 3 kcal/mol higher than that in PTP1B. This is consistent with the experimental data since the known inhibitory activity of compound VI against YopH is 30 μM (IC_{50}), while it is $K_i = 1.8$ nM against PTP1B. Compound VI is the most potent selective PTP1B inhibitor reported to date. Therefore, AutoDock is able to predict the selectivity among PTPs, providing a useful tool in the structure-based design and lead optimization of PTP inhibitors.

Using the same strategy, compound VI was docked to a pool of 500 MD conformers of SptP. Fig. 6C shows the most energetically stable conformation of compound VI bound in SptP. In contrast to the binding modes in YopH and PTP1B, the Asp linker of compound VI interacted with Gln380 and

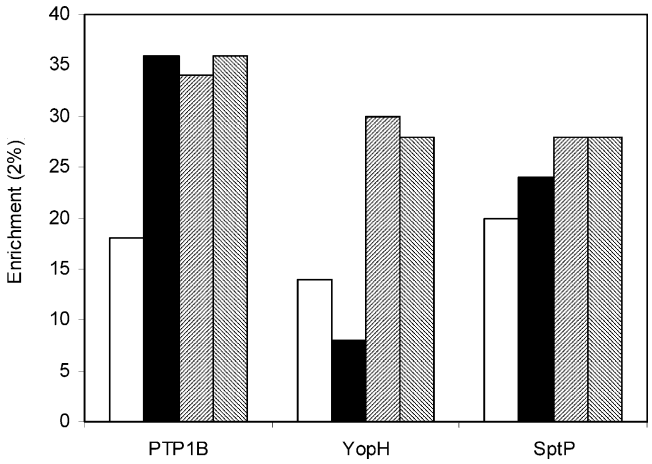

Fig. 7. Enrichments (2%) associated with different conformations of three PTPs (PTP1B, YopH, and SptP). The blank bars denote apo structure (open form), the black bars denote the X-ray structures in complex with inhibitor (closed form), and the pattern bars denote the structures selected from molecular dynamics simulations.

Lys384, and the distal 4-phosphonodifluoromethyl phenylacetyl group extended to a proximal site defined by Arg309, Lys384, Gln385, and Lys351. Significant movements were observed with these residues to make interactions with compound VI. The predicted binding energies of compound VI in SptP are −11.02 kcal/mol, higher than those in PTP1B and YopH.

3.7. Screening for PTP inhibitors by high throughput docking

The high throughput docking of 5000 compounds with 25 seeded inhibitors was performed on the three target proteins of PTP1B, YopH, and SptP using FlexX, a widely used virtual screening program [29]. In order to examine the effect of conformational changes of PTPs in the high throughput docking, several protein conformations including the apo structure with open binding pocket were used. Conformations obtained from molecular dynamics simulation in complex with compound III and compound VI were also adopted in docking. The screening efficiency was evaluated in terms of enrichment of the known inhibitors being pulled out from the random compounds.

The enrichments associated with different conformations of each protein showed significant differences (Fig. 7). The enrichments over 2% of the total compounds varied between 8 and 36. The highest enrichments were obtained for the three targets in complex with inhibitors 36, 30, and 28, respectively, indicating that these structures that incorporate protein conformational changes upon ligand binding are more suitable to high throughput docking. Compared to the closed form, the apo structure with open active site is less effective in the screening for selective pTyr mimetics. The enrichments associated with the three open conformations are significantly lower than those with the closed form.

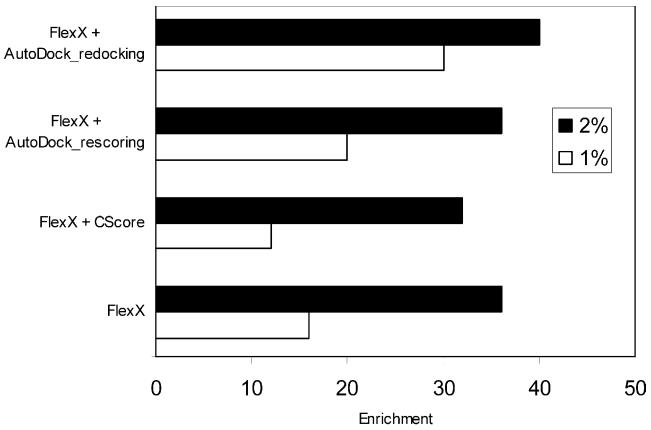

Fig. 8. Enrichments of PTP1B inhibitors using four approaches. The X-ray structure of PTP1B (1pty) is used in the virtual screening.

Visual examination of the docking poses showed that there were a number of "false positive" compounds docked in the active binding pocket. Most of seeded PTP inhibitors did not rank at the top of the hit-list. However, for those known "open form" inhibitors such as compound IV and compound V, they were not predicted using closed structure due to the failure of docking into the binding pocket.

The binding energies of the seeded PTP1B inhibitors predicted by FlexX showed a poor correlation to the experimental data. The correlation of experimental affinities verses the estimated binding energies was only 0.32. In comparison, the R^2 for AutoDock was 0.80, indicating a relatively high accuracy of the AutoDock free energy scoring function. Therefore, we applied a two-step docking in order to improve the screening efficiency. After initial docking using FlexX, the top 5% of the compounds were extracted from the FlexX docking and re-docked using AutoDock. The results were also compared with other two methods, re-scoring using AutoDock scoring function and consensus scoring using Cscore [31]. As illustrated in Fig. 8, significant improvement was obtained with the AutoDock re-docking after FlexX extraction. The enrichment over 1% of total compounds was increased from 16 to 30, but only to 20 when using the AutoDock scoring function to rescore the FlexX-generated poses. Using CScore to re-score the FlexX docking did not improve the screening efficiency, and we observed a slight decrease in performance in this case.

4. Discussion

4.1. Implications for structure-based design of YopH and SptP inhibitors

The design of selective PTP inhibitors has been a challenging problem because of the highly conserved active site shared by all PTPs. Probing the structural differences of YopH and SptP with respect to PTP1B at the active site as

well as the proximal binding sites offers a great opportunity in the structure-based drug design for the two bacterial protein tyrosine phosphatases. A distinct structural feature of YopH is that of an Arg404 at the active site playing an important role in ligand binding. A neutral residue Ser216 and a nonpolar Leu482 are present at this position for PTP1B and SptP, respectively. Compounds interacting with Arg404 at the active site in YopH appear to be more potent. In addition, a Gln357 is replaced the "sandwich" aromatic residue PTP1B Phe182 at the WPD loop, together with the conserved Gln446 in YopH, is more preferable to H-bonding and polar interactions with a ligand. These structural differences suggest that PTP selectivity could be achieved even with small molecules bound in the conserved active site. In fact, a crystal structure of YopH in complex with *p*-nitrocatechol (pNCS), the only known structure of YopH in complex with a small molecule (released during our docking studies), does show that Arg404 plays a crucial role in specific interactions with pNCS. Mutation of Arg404 to a Ser reduced the affinity of YopH for pNCS by 27-fold [32].

The second phosphate binding site is more intriguing in the development of selective PTP1B inhibitors [17]. YopH also possess a second phosphate binding site that allows simultaneous interactions of an inhibitor at both the active site and an adjacent peripheral site. Like PTP1B, YopH has most of the key residues in the second site, such as Arg205, Arg437, and the gateway residue Gly442. A difference is that YopH has a Gln443 at the position Met258 of PTP1B, and the second phosphate binding site in YopH exhibits a different molecular surface shape and charge distribution. SptP lacks such a characterized site. As shown in Fig. 9, the loop (SptP L7) that precedes such a helix in PTP1B and YopH turns away from the phosphatase in SptP and links directly to the GAP domain. However, the docking results revealed that the region defined by residues Phe310, Arg309, and Gln385 in SptP may provide an alternative site that is capable of interacting with a second functional group. Another important structural feature in PTP1B is the YRD motif. YopH has a similar motif of FRD at this position. The residue Phe229 functions in a manner same as PTP1B Tyr46 by participating in π–π interactions with the aromatic substrate; Arg230 and Asp231 form a very flexible region protruding out the catalytic binding pocket, allowing selectivity to be made over many other PTPs. In contrast, two uncharged serine residues in SptP occupy the positions of Arg and Asp. Molecular dynamics simulation showed that

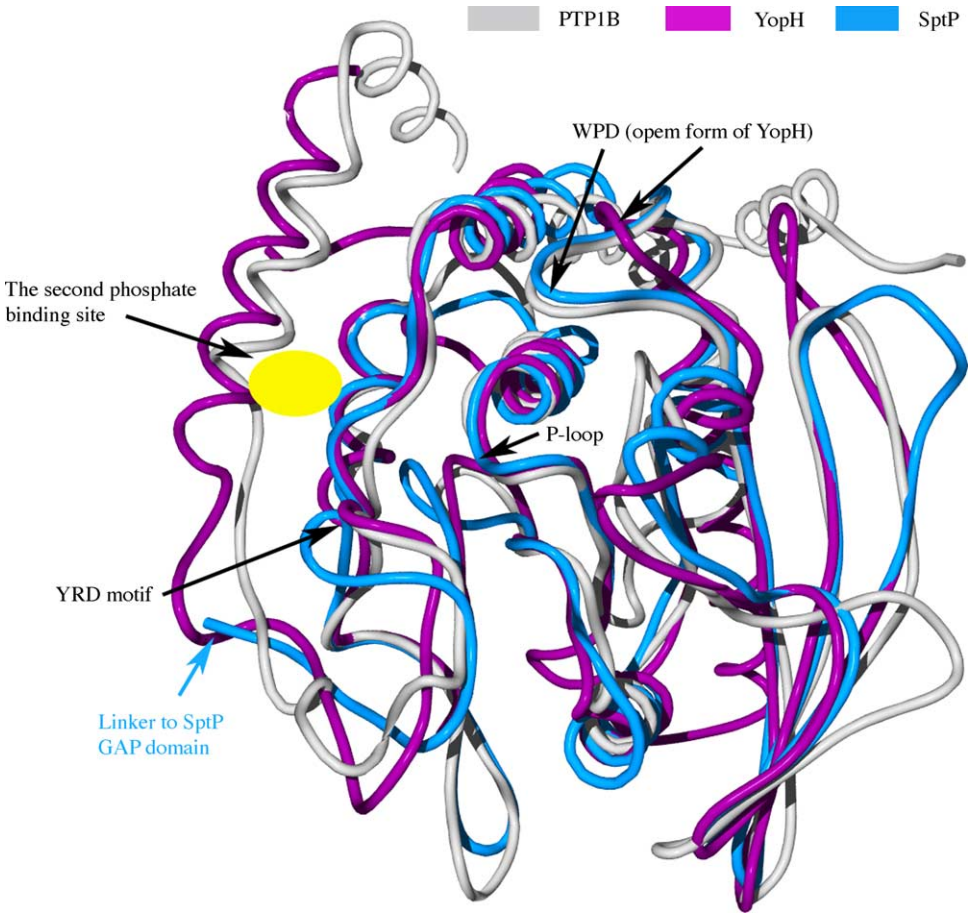

Fig. 9. Structural alignment of PTP1B with YopH and SptP phosphatase domain. Characterized binding sites are labeled.

this site is rather restricted and stable in SptP, probably due to the interactions that link the PTP and GAP domains [10].

4.2. Applications in virtual screening for selective PTP inhibitors

The scoring function and protein flexibility remain two critical issues in docking, and concerns with computational time generally restrict the use of sophisticated molecular mechanics energy functions and multiple protein structures in high throughput docking for database screening [33–35]. By several tools of assessment, AutoDock is shown to be more reliable in achieving accurate docking than FlexX, but it is also the most time-consuming approach (10–20 min in average in our study). FlexX uses a fast incremental construction searching method and empirical scoring function, providing the advantage of high speed (1–2 min per docking). In practice, we use a two-step docking strategy to improve the screening efficiency in the large database screening for PTP inhibitors. A rough docking is first performed using FlexX, and the top 5% compounds are extracted and re-docked using AutoDock. Compared to a simple re-scoring of the FlexX-generated poses using AutoDock scoring function, or the commonly used consensus scoring, the two-step docking is more efficient and robust, as well as with a reasonable speed. A possible explanation of this phenomenon is that there are many wrong-docked poses in FlexX docking, and re-scoring unlikely docked conformations cannot be expected to predict affinity reliably. We use a cutoff of 5% for the FlexX docking because more than 80% of active compounds could be extracted within the top 5% of FlexX-generated poses. When embarking in a database screening of more than 200,000 compounds, one is typically limited to visually inspecting 1% or less of the total compounds that ranked on the top of hit-list. Therefore, the improvement of 1% enrichment by AutoDock re-docking is significant in saving time and enhancing the probability of finding potential leads.

An unexpected result that the highest resolution structure of YopH (1lyv) gave the worst enrichment in virtual screening suggests that careful examination of conformational changes, especially the movements of WPD loop, should be made in the selection of protein structure of PTPs for docking. In general, the ligand-induced conformation of PTPs with WPD closed form is more suitable to the structure-based inhibitor design. However, the use of the apo structure can improve the chance of finding diverse hits with novel pTyr mimetics. In the docking of six selected compounds with AutoDock, we incorporated protein flexibility by sampling multiple protein conformations from molecular dynamics simulation. The use of a large number of conformations in database virtual screening is not currently practical, however. In this respect, a selection of a minimal set of representative conformations based on clustering or ligand docking should be a compromise yielding an efficient manner by which to deal with contributions of protein flexibility [36,37].

5. Conclusions

In summary, we have performed a comparative docking study of the *Yersinia* protein tyrosine phosphatase (PTP) YopH and the *Salmonella* PTP SptP with respect to the human PTP1B. Detailed analysis of the binding modes and binding energies has revealed common binding interactions in the three PTPs, and also distinguished characteristics observed in YopH and SptP that could impart inhibitory selectivity. A structural framework of the active site as well as adjacent peripheral sites that show potential for inhibitor design is provided. Furthermore, we have identified two docking approaches, AutoDock and FlexX, which when combined together, can be used efficiently in exploring the binding conformations of PTP inhibitor as well as in database virtual screening for potential leads. These results provide insight into the structure-based design for inhibitors of YopH and SptP as novel antibacterial drugs.

Acknowledgements

We thank R. Bennett, C. Pepper, A. Gazes, and G. Latter of the Rockefeller University Information Technology Resource Center for computational facilities. This work was funded in part by program grant 1U19AI056510-01 from the National Institute of Allergy and Infectious Disease.

References

[1] R.R. Brubaker, Factors promoting acute and chronic diseases caused by Yersiniae, Clin. Microbiol. Rev. 4 (1991) 309–324.
[2] T. Pang, M.M. Levine, B. Ivanoff, J. Wain, B.B. Finlay, Typhoid fever—important issues still remain, Trends Microbiol. 6 (1998) 131–133.
[3] M.L. Cohen, Changing patterns of infectious disease, Nature 406 (2000) 762–767.
[4] T.V. Inglesby, D.T. Dennis, D.A. Henderson, J.G. Bartlett, M.S. Ascher, E. Eitzen, A.D. Fine, A.M. Friedlander, J. Hauer, J.F. Koerner, M. Layton, J. McDade, M.T. Osterholm, T. O'Toole, G. Parker, T.M. Perl, P.K. Russell, M. Schoch-Spana, K. Tonat, Plague as a biological weapon: medical and public health management. Working group on civilian biodefense, J. Am. Med. Assoc. 283 (2000) 2281–2290.
[5] R.J. Hawley, E.M. Eitzen Jr., Biological weapons—a primer for microbiologists, Annu. Rev. Microbiol. 55 (2001) 235–253.
[6] G.R. Cornelis, F. Van Gijsegem, Assembly and function of type III secretory systems, Annu. Rev. Microbiol. 54 (2000) 735–774.
[7] G.R. Cornelis, The Yersinia Yop virulon, a bacterial system to subvert cells of the primary host defense, Folia Microbiol. (Praha) 43 (1998) 253–261.
[8] D.S. Black, J.B. Bliska, Identification of p130cas as a substrate of Yersinia yoph (Yop51), a bacterial protein tyrosine phosphatase that translocates into mammalian cells and targets focal adhesions, EMBO J. 16 (1997) 2730–2744.

[9] J.E. Galan, Salmonella interactions with host cells: type III secretion at work, Annu. Rev. Cell Dev. Biol. 17 (2001) 53–86.
[10] C.E. Stebbins, J.E. Galan, Modulation of host signaling by a bacterial mimic: structure of the salmonella effector SptP bound to Rac1, Mol. Cell 6 (2000) 1449–1460.
[11] Z.Y. Zhang, Protein tyrosine phosphatases: prospects for therapeutics, Curr. Opin. Chem. Biol. 5 (2001) 416–423.
[12] R.H. van Huijsduijnen, A. Bombrun, D. Swinnen, Selecting protein tyrosine phosphatases as drug targets, Drug Discov. Today 7 (2002) 1013–1019.
[13] E.A. Harley, N. Levens, Protein tyrosine phosphatase 1B inhibitors for the treatment of type 2 diabetes and obesity: recent advances, Curr. Opin. Investig. Drugs 4 (2003) 1179–1189.
[14] M.A. Blaskovich, H.O. Kim, Recent discovery and development of protein tyrosine phosphatase inhibitors, Expert Opin. Ther. Pat. 12 (2002) 871–905.
[15] Z.Y. Zhang, Protein tyrosine phosphatases: structure and function, substrate specificity, and inhibitor development, Annu. Rev. Pharmacol. Toxicol. 42 (2002) 209–234.
[16] T.R. Burke Jr., Z.Y. Zhang, Protein-tyrosine phosphatases: structure, mechanism, and inhibitor discovery, Biopolymers 47 (1998) 225–241.
[17] M. Sarmiento, L. Wu, Y.F. Keng, L. Song, Z. Luo, Z. Huang, G.Z. Wu, A.K. Yuan, Z.Y. Zhang, Structure-based discovery of small molecule inhibitors targeted to protein tyrosine phosphatase 1B, J. Med. Chem. 43 (2000) 146–155.
[18] T.O. Johnson, J. Ermolieff, M.R. Jirousek, Protein tyrosine phosphatase 1B inhibitors for diabetes, Nat. Rev. Drug Discov. 1 (2002) 696–709.
[19] J.P. Sun, A.A. Fedorov, S.Y. Lee, X.L. Guo, K. Shen, D.S. Lawrence, S.C. Almo, Z.Y. Zhang, Crystal structure of PTP1B complexed with a potent and selective bidentate inhibitor, J. Biol. Chem. 278 (2003) 12406–12414.
[20] X.L. Guo, K. Shen, F. Wang, D.S. Lawrence, Z.Y. Zhang, Probing the molecular basis for potent and selective protein-tyrosine phosphatase 1B inhibition, J. Biol. Chem. 277 (2002) 41014–41022.
[21] B.G. Szczepankiewicz, G. Liu, P.J. Hajduk, C. Abad-Zapatero, Z. Pei, Z. Xin, T.H. Lubben, J.M. Trevillyan, M.A. Stashko, S.J. Ballaron, H. Liang, F. Huang, C.W. Hutchins, S.W. Fesik, M.R. Jirousek, Discovery of a potent, selective protein tyrosine phosphatase 1B inhibitor using a linked-fragment strategy, J. Am. Chem. Soc. 125 (2003) 4087–4096.
[22] Y.A. Puius, Y. Zhao, M. Sullivan, D.S. Lawrence, S.C. Almo, Z.Y. Zhang, Identification of a second aryl phosphate-binding site in protein-tyrosine phosphatase 1B: a paradigm for inhibitor design, Proc. Natl. Acad. Sci. U.S.A. 94 (1997) 13420–13425.
[23] L.F. Iversen, H.S. Andersen, S. Branner, S.B. Mortensen, G.H. Peters, K. Norris, O.H. Olsen, C.B. Jeppesen, B.F. Lundt, W. Ripka, K.B. Moller, N.P. Moller, Structure-based design of a low molecular weight, nonphosphorus, nonpeptide, and highly selective inhibitor of protein-tyrosine phosphatase 1B, J. Biol. Chem. 275 (2000) 10300–10307.
[24] SYBYL Molecular Modeling Software, V6.9; Tripos Associates, St. Louis, MO.
[25] H.M. Berman, J. Westbrook, Z. Feng, G. Gilliland, T.N. Bhat, H. Weissig, I.N. Shindyalov, P.E. Bourne, The protein data bank, Nucleic Acids Res. 28 (2000) 235–242.
[26] G.M. Morris, D.S. Goodsell, R.S. Halliday, R. Huey, W.E. Hart, R.K. Belew, A.J. Olson, Automated docking using a lamarckian genetic algorithm and an empirical binding free energy function, J. Comput. Chem. 19 (1998) 1639–1662.
[27] J. Gasteiger, M. Marsili, Iterative partial equalization of orbital electronegativity—a rapid access to atomic charges, Tetrahedron 36 (1980) 3219–3228.
[28] J.P. Ryckaert, G. Ciccotti, H.J.C. Berendsen, Numerical-integration of cartesian equations of motion of a system with constraints—molecular-dynamics of *n*-alkanes, J. Comput. Phys. 23 (1977) 327–341.
[29] M. Rarey, B. Kramer, T. Lengauer, G. Klebe, A fast flexible docking method using an incremental construction algorithm, J. Mol. Biol. 261 (1996) 470–489.
[30] L.F. Iversen, H.S. Andersen, K.B. Moller, O.H. Olsen, G.H. Peters, S. Branner, S.B. Mortensen, T.K. Hansen, J. Lau, Y. Ge, D.D. Holsworth, M.J. Newman, N.P. Hundahl Moller, Steric hindrance as a basis for structure-based design of selective inhibitors of protein-tyrosine phosphatases, Biochemistry 40 (2001) 14812–14820.
[31] P.S. Charifson, J.J. Corkery, M.A. Murcko, W.P. Walters, Consensus scoring: a method for obtaining improved hit rates from docking databases of three-dimensional structures into proteins, J. Med. Chem. 42 (1999) 5100–5109.
[32] J.P. Sun, L. Wu, A.A. Fedorov, S.C. Almo, Z.Y. Zhang, Crystal structure of the yersinia protein-tyrosine phosphatase YopH complexed with a specific small molecule inhibitor, J. Biol. Chem. 278 (2003) 33392–33399.
[33] H.A. Carlson, J.A. McCammon, Accommodating protein flexibility in computational drug design, Mol. Pharmacol. 57 (2000) 213–218.
[34] S.J. Teague, Implications of protein flexibility for drug discovery, Nat. Rev. Drug Discov. 2 (2003) 527–541.
[35] X. Hu, S. Balaz, W.H. Shelver, A practical approach to docking of zinc metalloproteinase inhibitors, J. Mol. Graph. Model. 22 (2004) 293–307.
[36] J. Varady, X. Wu, X. Fang, J. Min, Z. Hu, B. Levant, S. Wang, Molecular modeling of the three-dimensional structure of dopamine 3 (D3) subtype receptor: discovery of novel and potent D3 ligands through a hybrid pharmacophore- and structure-based database searching approach, J. Med. Chem. 46 (2003) 4377–4392.
[37] S. Yoon, W.J. Welsh, Identification of a minimal subset of receptor conformations for improved multiple conformation docking and two-step scoring, J. Chem. Inf. Comput. Sci. 44 (2004) 88–96.